

Priority communication

# A characterization study of some aspects of the adsorption of aqueous $\text{Co}^{2+}$ ions on a natural bentonite clay

T. Shahwan<sup>a,\*</sup>, H.N. Erten<sup>b</sup>, S. Unugur<sup>b</sup>

<sup>a</sup> Department of Chemistry, Izmir Institute of Technology, 35430 Urla, Izmir, Turkey

<sup>b</sup> Department of Chemistry, Bilkent University, 06800 Bilkent, Ankara, Turkey

Received 21 March 2006; accepted 22 April 2006

Available online 13 June 2006

## Abstract

The natural bentonite used in this study contained montmorillonite in addition to low cristobalite. The uptake of aqueous  $\text{Co}^{2+}$  ions was investigated as a function of time, concentration, and temperature. In addition, the change in the interlayer space of montmorillonite was analyzed using XRPD, and the distribution of fixed  $\text{Co}^{2+}$  ions on the heterogeneous clay surface was recorded using EDS mapping. The sorbed amount of  $\text{Co}^{2+}$  appeared to closely follow Freundlich isotherm, with the sorption process showing apparent endothermic behavior. The relevance of the apparent  $\Delta H^{\circ}$  values is briefly discussed. Analysis of the Co-sorbed bentonite samples using SEM/EDS showed that the montmorillonite fraction in the mineral was more effective in  $\text{Co}^{2+}$  fixation than the cristobalite fraction. XRPD analysis demonstrated that the interlayer space of montmorillonite was slightly modified at the end of sorption.

© 2006 Elsevier Inc. All rights reserved.

**Keywords:**  $\text{Co}^{2+}$ ; Bentonite; Adsorption

## 1. Introduction

$^{60}\text{Co}$  ( $t_{1/2} = 5.27$  yr) is an important radioisotope of Co that is extensively used in medicine for cancer treatment and sterilization. This radioisotope is produced by nuclear activation of  $^{59}\text{Co}$  in nuclear power plants. Due to its relatively long half-life and strong  $\gamma$  radiation ( $E_{\gamma} = 1173.2, 1332.5$  keV),  $^{60}\text{Co}$  is an important radionuclide to watch for from the viewpoint of environmental safety, in particular if this element is present in its aqueous ionic form, which facilitates its migration within terrestrial systems.

Bentonite is the name of the rock that contains the montmorillonite type of clay minerals. Compared with other clay types, montmorillonite has excellent sorption properties and possesses sorption sites available within its interlayer space as well as on the outer surface and edges. Montmorillonite belongs to the 2:1 clay family, the basic structural unit of which is composed of two tetrahedrally coordinated sheets of silicon ions surrounding

a sandwiched octahedrally coordinated sheet of aluminum ions. The binding force between the stacked layers of basic units is mainly the weak van der Waals type of force, which facilitates change in the interlayer space size depending on the humidity conditions and/or the type of material encountered within the interlayer spacing of the clay. Montmorillonite is usually subjected to isomorphous substitution (e.g., substitution of  $\text{Mg}^{2+}$  for  $\text{Al}^{3+}$ ), thus leading to the development of a negative charge on the entire structure.

According to our literature survey results, a limited number of studies regarding the sorption of  $\text{Co}^{2+}$  on bentonite are available. The reported studies have addressed the effects of various parameters on the extent and nature of uptake of  $\text{Co}^{2+}$  by bentonite (or montmorillonite). The effects of pH and chelating agents were investigated and they were reported to substantially affect the retarded  $\text{Co}^{2+}$  ions [1,2]. Thermodynamic aspects of  $\text{Co}^{2+}$  retention by bentonite have also been discussed in other works [3,4]. These studies reported concentration-dependent sorption that is nonlinear and of an endothermic nature. Another study has noted that  $\text{Co}^{2+}$  sorption is time-dependent and highly irreversible [5]. High affinity of Na-activated bentonite for  $\text{Co}^{2+}$  was reported and the effect of solid/liquid ratio on the

\* Corresponding author. Fax: +90 232 750 7509.

E-mail address: [talalshahwan@iyte.edu.tr](mailto:talalshahwan@iyte.edu.tr) (T. Shahwan).

sorption process was discussed in another work [6]. The analytical applicability of bentonite in the preconcentration of  $\text{Co}^{2+}$  contained in waste water (prior to analysis by atomic absorption spectroscopy) was verified [7].

In this study, various aspects of the sorption behavior of  $\text{Co}^{2+}$  on this clay were examined. Part of the experiments were performed using  $^{60}\text{Co}$  as a radiotracer, while in the other part only stable Co isotopes were applied, with the bulk concentration of cobalt in this part determined using atomic absorption spectroscopy (AAS). The investigated sorption parameters were the effects of time, concentration, and temperature. Characterization of the natural and Co-loaded bentonite samples was done using scanning electron microscopy–energy-dispersive X-ray spectroscopy (SEM/EDS) in addition to X-ray powder diffraction (XRPD). SEM/EDS was applied to reveal the distribution of  $\text{Co}^{2+}$  across the heterogeneous bentonite surface, while XRPD analysis aimed at studying any structural changes in the bentonite matrix upon  $\text{Co}^{2+}$  sorption.

## 2. Experimental

The bentonite samples originated from the Giresun region, located on the Black Sea coast of Turkey. The samples were dry-sieved and the fractions with particle size  $<38\ \mu\text{m}$  were used in the experiments. Throughout the study, the batch method was applied. To each of a set of 50-mg bentonite samples placed in preweighed tubes, 5.0 ml of  $\text{Co}^{2+}$  solution (prepared from cobalt nitrate salt) containing an appropriate amount of  $^{60}\text{Co}$  radiotracer was added. The initial concentrations of  $\text{Co}^{2+}$  solution used in these experiments were 100, 500, 1000, and 2500 mg/L. Tubes were shaken at temperatures of  $25\ ^\circ\text{C}$  for time periods of 10 min, 30 min, 2 h, 4 h, 7 h, 24 h, 48 h, and 4 days. The experiments were then repeated at  $55\ ^\circ\text{C}$  for the initial concentrations 750, 1000, 1500, and 2500 mg/L. Shaking was done in a temperature-controlled environment using a Nuve ST 402 water bath shaker equipped with a microprocessor thermostat. The samples were then centrifuged and 4.0-ml portions of the supernatant were counted for 1000 s using a  $35\text{-cm}^3$  HPGc detector connected to a multichannel PGT analyzer. Duplicate samples were used in each measurement.

The pH of the cobalt solutions in contact with bentonite varied between 4.2 and 6.4, with the pH decreasing as the initial concentration was increased. The chemical speciation analysis of cobalt ions in aqueous solution under different pH conditions was performed using visual MINTEQ software. The data were generated based on the initial concentration, temperature, pH, and ionic strength, all of which were defined in an input file. According to this analysis, up to pH values of 8–9, the dominant chemical form of Co in aqueous media is  $\text{Co}^{2+}$ . Beyond pH 9, other forms of Co (such as  $\text{CoOH}^+$  and  $\text{Co}(\text{OH})_2(\text{aq})$ ) become increasingly effective. Based on this analysis, it is clear that within the experimental conditions of this study, the dominant form of cobalt in aqueous media is  $\text{Co}^{2+}$ .

In the Co-loaded bentonite samples that were characterized by surface techniques, no radioactive cobalt was used. The SEM/EDS analysis was started by sprinkling the solid samples

onto adhesive carbon taps supported by circular metallic disks. The samples were then analyzed using a Philips XL-30S FEG type SEM/EDS instrument. Images of the sample surfaces were recorded at different magnifications. EDS elemental analysis was performed at several different points of the surface in order to minimize any possible anomalies arising from the heterogeneous nature of the analyzed surface.

The natural and Co-sorbed bentonite samples were also characterized using XRPD. For this purpose, the powders were first ground, mounted on rectangular glass holders, and then introduced to a Rigaku miniflex instrument for X-ray diffraction analysis.  $\text{CuK}\alpha$  radiation was used as a source. X-rays were generated in a tube operating at 30 kV and 15 mA. Spectra were recorded with  $2\theta$  values ranging from  $2$  to  $35^\circ$  in steps of  $0.02^\circ$  and dwell times of 10 s per step.

## 3. Results and discussion

The XRPD pattern of natural bentonite is given in Fig. 1a. The figure indicates that the clay is composed primarily of montmorillonite, with the characteristic features at  $d_{001} = 15.15\ \text{\AA}$  and  $d_{020} = 4.50\ \text{\AA}$ , in addition to low cristobalite (a polymorph of quartz), marked by its main reflection at  $d_{101} = 4.05\ \text{\AA}$ . The heterogeneous nature of the natural clay is demonstrated in the SEM image given in Fig. 1b. The elemental composition of bentonite obtained using EDS showed that the atomic percentages are 57.3 (O), 31.1 (Si), 8.1 (Al),

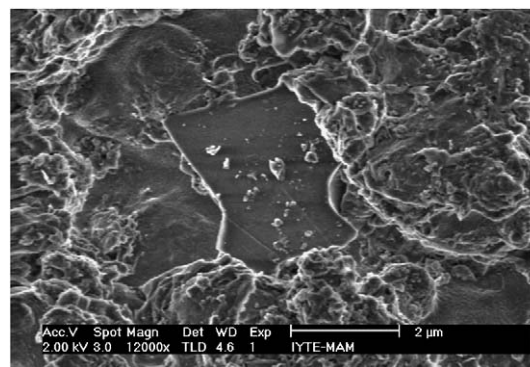
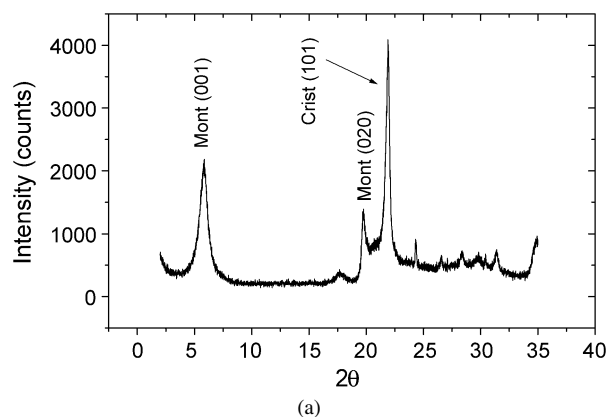


Fig. 1. (a) XRPD pattern of bentonite mineral applied in this study; (b) a typical SEM image of the surface of the same mineral.

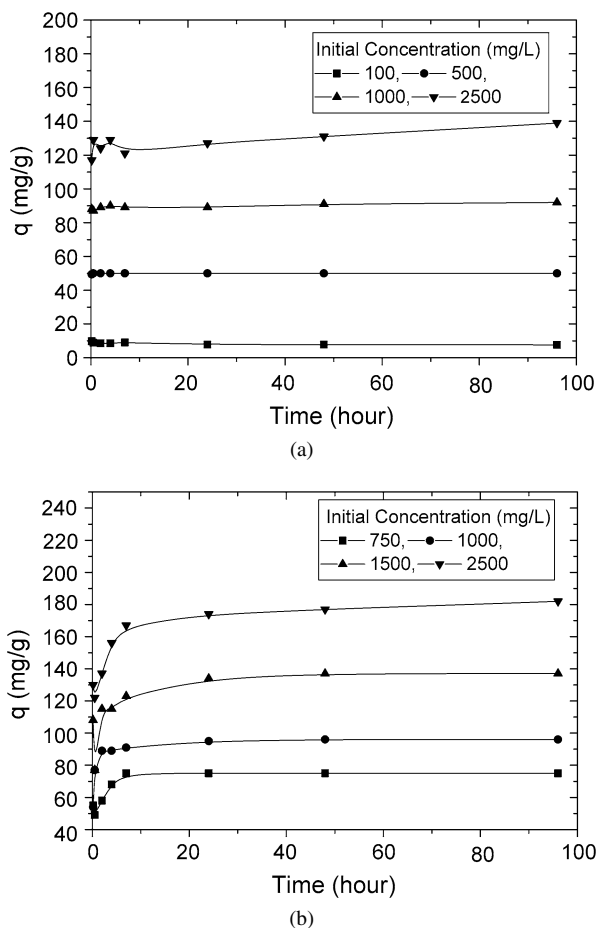


Fig. 2. Variation of the sorbed amounts of  $\text{Co}^{2+}$  (mg/g) as a function of time at (a) 25 °C, (b) 55 °C.

and 2.3 (Mg), in addition to minimal amounts of Ca, Na, and Fe.

### 3.1. Kinetic analysis

The results of the kinetic experiments performed at 25 °C (Fig. 2a) showed that equilibrium is attained within the first few hours of mixing at initial concentrations of 100, 500, and 1000 mg/L, while more than 2 days is required to approach equilibrium at the initial concentration of 2500 mg/L. The kinetic experiments were repeated at 55 °C for initial concentrations 750, 1000, 1500, and 2500 mg/L. The results are shown in Fig. 2b. As demonstrated by the figure, the increase in temperature is causing a delay in the attainment of equilibrium, revealed by comparing the curves corresponding to initial concentrations of 1000 and 2500 mg/L in Figs. 2a and 2b, although the sorbed amount of  $\text{Co}^{2+}$  increases. From a physicochemical perspective, the rate constant is expected to usually increase as the temperature is increased [8], but it must be noted that this is based on the behavior of gases, where the increase in temperature, in a medium in which the intermolecular forces are very weak, leads to an increase in the kinetic energy of gas molecules/atoms and thus enhances the rate of reactions. In liquid–solid systems, however, the situation is much more

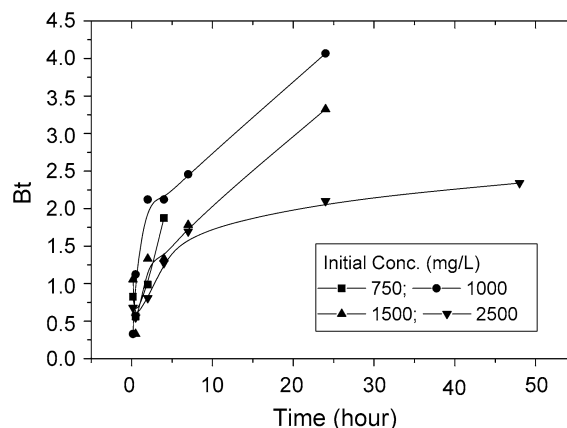


Fig. 3. Boyd plots of the sorption data at 55 °C at different initial concentrations.

complex and the behavior of ions in solution or on the solid, as temperature is increased, will be subject to factors such as the interionic forces, the hydration energy, the availability of sorption sites, and the relative stability of sorbed ions at these sites.

For the intrinsic sorption reaction of  $\text{Co}^{2+}$  ions to take place, these ions must first diffuse through the aqueous film surrounding the clay particle and then undergo an intraparticle diffusion step (through the interlayer of montmorillonite) before they reach the sorption site. Here it is implicitly assumed that sorption occurs primarily on the interlayer sites of montmorillonite, a clay with expandable interlayers. The sorption data that showed variation with time (those corresponding to  $T = 55$  °C) were used in testing whether film diffusion or intraparticle diffusion is the rate-determining step. For this purpose, the Boyd equation was applied. This equation is given by [9]

$$F = 1 - \frac{6}{\pi^2} \exp(-Bt), \quad (1)$$

where  $F$  is the fraction of solute sorbed at any time  $t$  (i.e.,  $q/q_e$ ), and  $Bt$  is a mathematical function of  $F$ . Rearranging the above equation gives

$$Bt = -0.4977 - \ln(1 - F). \quad (2)$$

Hence, the values of  $Bt$  can be calculated at each different coverage and then plotted against time. The relevant plots are used to test whether linear behavior is obtained and whether the lines pass through zero, which is useful in distinguishing between film diffusion and interlayer diffusion. The corresponding plots are shown in Fig. 3. The obtained curves demonstrate linear behavior at the initial stages of sorption. It is reported that if the lines do not pass through the origin during the initial steps of the sorption process, then external transport is the rate-limiting step [9]. This suggests that once  $\text{Co}^{2+}$  ions reach the interlayer region they rapidly diffuse through and attach to sorption sites.

### 3.2. Sorption equilibria and isotherms

The sorption data corresponding to equilibrium conditions were expressed in terms of the distribution ratio ( $R_d =$

Table 1  
Values of  $[C]_s$ , distribution ratio  $R_d$  and percentage sorption (PS) of  $\text{Co}^{2+}$  ions on bentonite when equilibrium is approached

298 K				328 K			
$[C]_o$ (mg/L)	$[C]_s$ (mg/g)	$R_d$ (ml/g)	PS	$[C]_o$ (mg/L)	$[C]_s$ (mg/g)	$R_d$ (ml/g)	PS
100	9.7	2841	97	750	69.1	1156	92
500	47.1	1595	94	1000	89.6	787	89
1000	83.1	490	83	1500	125.9	391	79
2500	139.3	154	64	2500	181.3	250	71

$[C]_s/[C]_l$ ) and the percentage sorption ( $\text{PS}/100 = 1 - [C]_l/[C]_o$ ). The  $[C]_s$  values were calculated using

$$[C]_s = ([C]_o - [C]_l)(V/M), \quad (3)$$

where  $V$  is the solution volume (L), and  $M$  is the mass of sorbent (g). The results corresponding to different initial concentrations are provided in Table 1. At both temperatures, increasing the initial concentration causes a decrease in both  $R_d$  and PS values, indicating a decrease in the number of available sorption sites with increased loading.

The data adequately obeyed a Freundlich isotherm model, which describes adsorption on solids possessing sites that might vary in their sorption energy, without any restriction on the sorption capacity of those solids. The isotherm model is given by

$$[C]_s = k[C]_l^n. \quad (4)$$

Here,  $[C]_s$  is the equilibrium concentration of the solute on the solid (mg/g),  $[C]_l$  is the equilibrium concentration of the solute in the liquid phase (mg/L), and  $k$  and  $n$  are Freundlich constants. The plots of the sorption data corresponding to mixing periods of 48 h at temperatures of 25 and 55 °C are given in Fig. 4. According to the linear fits of the data, the values of  $n$  were 0.49 and 0.37, and those of  $k$  were 6.5 and 15.2 mg/g at temperatures of 25 and 55 °C, respectively. The values of  $n$  are indicative that the sorption process is significantly nonlinear, whereas the  $k$  values reflect the stronger affinity of the clay toward  $\text{Co}^{2+}$  ions at higher temperatures.

### 3.3. Thermodynamic parameters

The equilibrium data were applied in calculating the values of the thermodynamic parameters of sorption,  $\Delta H^\circ$ ,  $\Delta S^\circ$ , and  $\Delta G^\circ$  by the equations

$$\Delta H^\circ = R \ln \frac{R_d(T_2)}{R_d(T_1)} \left( \frac{T_1 T_2}{T_2 - T_1} \right), \quad (5)$$

$$\Delta S^\circ = \frac{\Delta H^\circ - \Delta G^\circ}{T}, \quad (6)$$

$$\Delta G^\circ = -RT \ln R_d. \quad (7)$$

The evaluation of the above thermodynamic parameters in sorption studies is subject to a number of limitations. One of the most important limitations is the fact that the  $R_d$  is not a thermodynamic equilibrium constant but merely an empirical constant that is valid under a particular set of reaction conditions. The

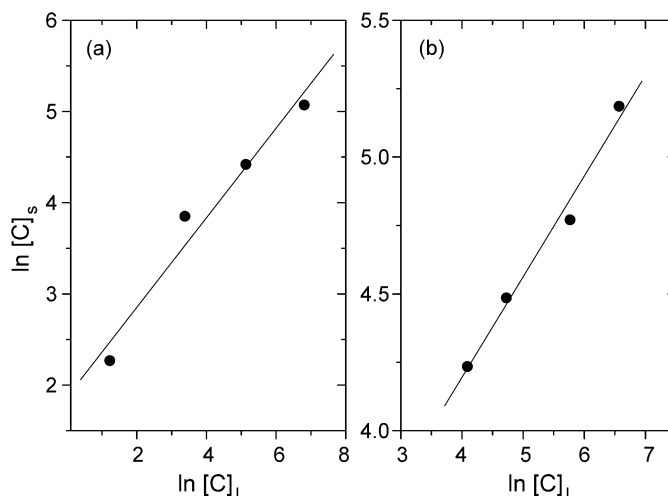


Fig. 4. Freundlich isotherms of  $\text{Co}^{2+}$  sorption data at (a)  $T = 25^\circ\text{C}$ , (b)  $T = 55^\circ\text{C}$ .

Table 2

Values of  $\Delta H^\circ$  (kJ/mol),  $\Delta S^\circ$  (J/mol K), and  $\Delta G^\circ$  (kJ/mol) calculated using the sorption data that correspond to initial concentrations of 1000 and 2500 mg/L at the studied temperatures of 25 and 55 °C for a mixing period of 96 h

$[C]_o$ (mg/L)	$\Delta H^\circ$ (kJ/mol)	$\Delta G^\circ$ (kJ/mol)		$\Delta S^\circ$ (J/mol K)	
		298 K	328 K	298 K	328 K
1000	12.8	-15.3	-12.5	94.3	77.1
2500	13.1	-18.2	-15.1	105.0	86.0
Average	13.0	-16.8	-13.8	99.7	81.6

dependence of  $R_d$  on the initial concentration is thus reflected in the calculated  $\Delta H^\circ$ ,  $\Delta S^\circ$ , and  $\Delta G^\circ$  values, which are—from a thermodynamic perspective—only temperature-dependent, as long as the external pressure is constant and the attainment of equilibrium ensures the equality of the chemical potential of the solute at both sides of the liquid/solid interface. Nevertheless, during the calculation of  $\Delta H^\circ$ ,  $\Delta S^\circ$ , and  $\Delta G^\circ$  values it is always assumed that these properties do not vary significantly over the applied range of temperatures.

$\Delta H^\circ$ ,  $\Delta S^\circ$ , and  $\Delta G^\circ$  values were calculated using the sorption data that correspond to the same initial concentrations (i.e., 1000 and 2500 mg/L) at both temperatures, 25 and 55 °C, for a mixing period of 96 h. The obtained values are provided in Table 2. The values corresponding to each of the two concentrations are given and an average of these values is calculated to provide an estimate of these thermodynamic properties over the entire range of initial concentrations. Negative  $\Delta G^\circ$  values indicate that the sorption process is preferentially driven toward the products. The values are well below those associated with chemical bond formation, indicating the physical nature of the sorption process. The entropy change of the system accompanying the fixation of  $\text{Co}^{2+}$  by bentonite comes out as positive, indicating that more disorder is generated in the system upon sorption. The increase in the disorder upon sorption was discussed in an earlier study [10]. The positive value of  $\Delta H^\circ$  marks the endothermic nature of sorption, i.e., that higher temperatures are favored for enhanced removal of  $\text{Co}^{2+}$  ions by

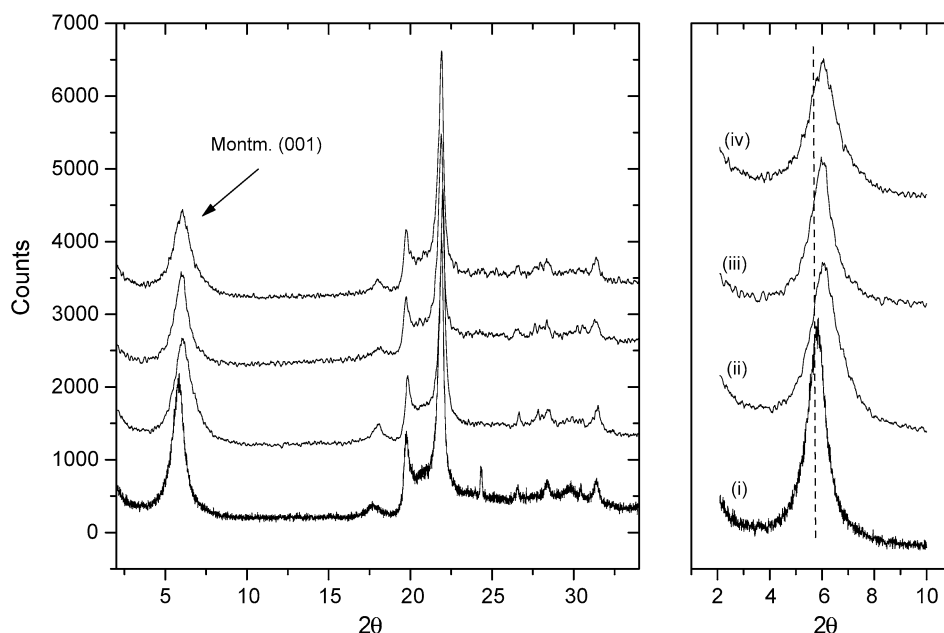


Fig. 5. XRPD patterns of bentonite before  $\text{Co}^{2+}$  sorption (i) and after  $\text{Co}^{2+}$  sorption at different initial concentrations (ii = 10, iii = 100, iv = 1000 mg/L).

bentonite. The endothermic nature and positive entropy change of  $\text{Co}^{2+}$  sorption by other types of bentonite have previously been reported [4,5].

The  $\Delta H^{\circ}$  values reported in Table 2 stand for the observed enthalpy change,  $\Delta H_{\text{obs}}^{\circ}$ , which includes the contribution of intrinsic enthalpy change,  $\Delta H_{\text{int}}^{\circ}$ , and the hydration enthalpy of the sorbate cation,  $\Delta H_{\text{hyd}}^{\circ}$ . These enthalpies can be related through the relation [11]  $\Delta H_{\text{obs}}^{\circ} = \Delta H_{\text{int}}^{\circ} - \Delta H_{\text{hyd}}^{\circ}$ . The intrinsic enthalpy change is associated with the fixation reaction of  $\text{Co}^{2+}$  ions on the sorption sites and is always exothermic, and the hydration enthalpy (exothermic) reflects the strength of interaction between the naked cation and its hydration sphere. Hence for the intrinsic sorption reaction to take place, the cation must first undergo partial dehydration in a way that facilitates its migration through the solution to the sites on the sorbent. Based on this and depending on some of our earlier studies, we may conclude, as a first approximation, that cations with relatively low hydration enthalpies (low charge/size ratio, e.g.,  $\text{Cs}^{+}$ ) will demonstrate observed exothermic sorption behavior [12], while cations of higher charge/size ratio (e.g.,  $\text{Sr}^{2+}$ ,  $\text{Co}^{2+}$ ) will generally show observed endothermic sorption behavior [4, 10]. Based on the above statements, the values of  $\Delta H_{\text{int}}^{\circ}$  could essentially be greater in magnitude than the reported values of  $\Delta H_{\text{obs}}^{\circ}$ .

#### 3.4. XRPD and SEM/EDS characterization of Co-sorbed bentonite

Another important point to consider is the dehydration of the clay itself upon sorption. Montmorillonite is known to be a swelling clay that contains water of hydration. The extent of hydration of the clay is dependent on the type and nature of interlayer cations, temperature, and pressure, in addition to its crystalline structure. Since the hydration state of montmoril-

lonite is expected to be reflected by the size of its interlayer space, the effect of  $\text{Co}^{2+}$  sorption on the basal space ( $d_{001}$ ) of montmorillonite was studied using XRPD. The XRPD patterns of the exchanged clay samples at various  $\text{Co}^{2+}$  initial concentrations of 10, 100, and 1000 mg/L (Fig. 5) indicated a decrease in the intensity and a slight shift in the position of the  $d_{001}$  peak from 15.15 to 14.49 Å ( $\pm 0.37$ , depending on the initial cobalt concentration). The reduction in the basal spacing of this feature could be indicative of a decrease in the number of water layers in the interlayer space as a consequence of the  $\text{Co}^{2+}$  sorption. It must be noted, however, that under the applied concentrations, we could not observe a systematic change in  $d_{001}$  of montmorillonite with increasing/decreasing concentration, and further consideration of this issue is required. In an earlier study, similar changes in the interlayer space were observed to accompany  $\text{Ba}^{2+}$  sorption by the same type of bentonite [13]. Other authors reported similar reductions in  $d_{001}$  of montmorillonite upon sorption of  $\text{Pb}^{2+}$  and  $\text{Zn}^{2+}$  and concluded that bulky polynuclear complexes such as the hydrolysis products do not form in the interlamellar space of the clay upon the sorption of these ions [14].

Multiple-spot EDS analysis has also revealed that the regions rich in cristobalite (understood from the fact that only Si and O peaks were observed at these regions) did not contain detectable amounts of  $\text{Co}^{2+}$ , unlike the regions rich in montmorillonite, which seemed to be richer in  $\text{Co}^{2+}$  content. This suggests that montmorillonite fractions in the bentonite mineral form a more preferable sink for  $\text{Co}^{2+}$  ions than cristobalite fractions. Typical EDS spectra that illustrate this observation are provided in Figs. 6a and 6b. Moreover, a typical EDS mapping image obtained from Co-loaded bentonite surface (area of  $100 \times 100 \mu\text{m}$ ) that shows the distribution of sorbed Co ( $K$  line) is also given in Fig. 6c. The localization of Co signals is evident from the image. The elemental composition provided as insets

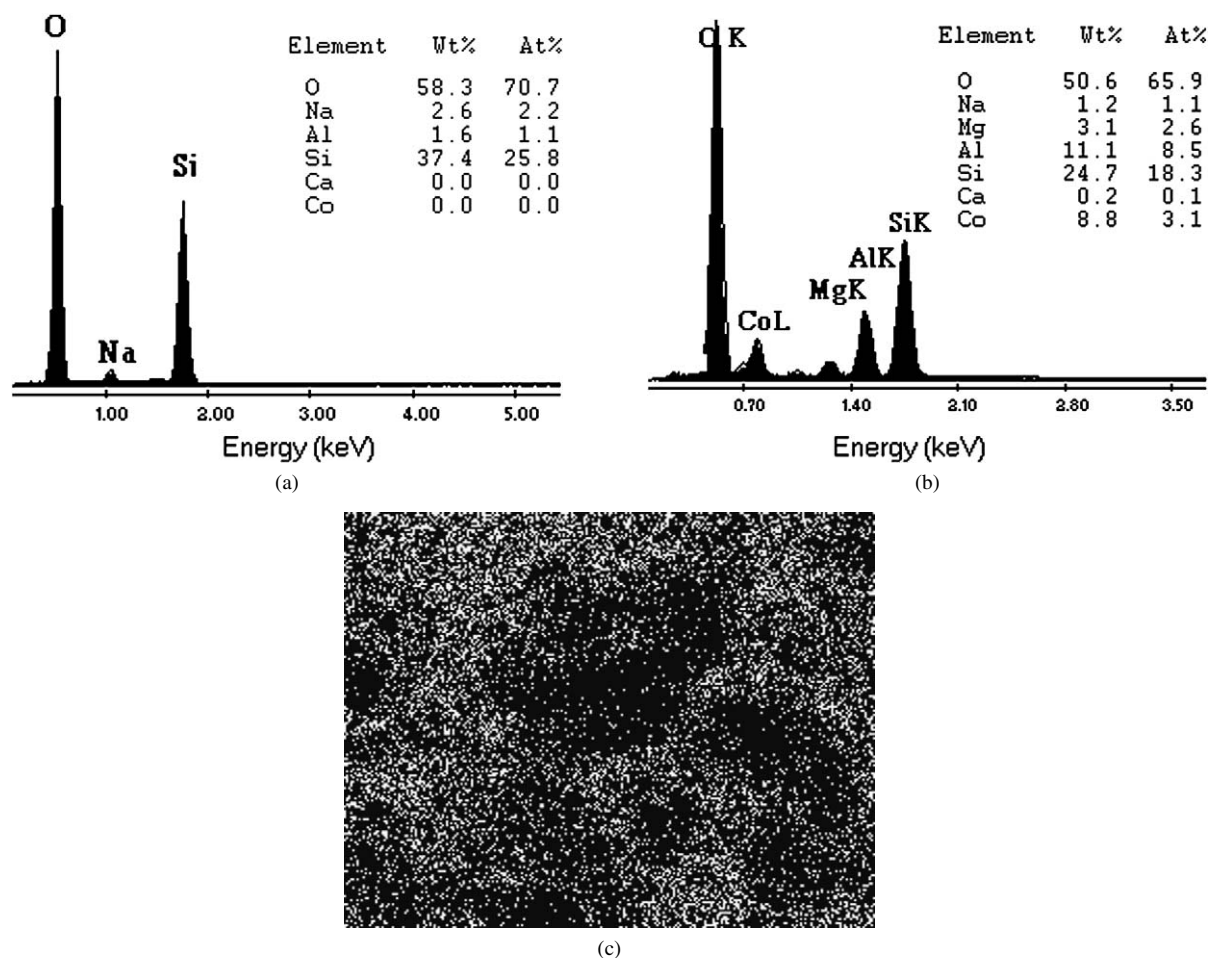


Fig. 6. (a) A typical EDS spectrum of a region rich in cristobalite; (b) a typical EDS spectrum of a region rich in montmorillonite; (c) a typical EDS mapping image showing the distribution of cobalt signals on the surface of bentonite (area of  $100 \times 100 \mu\text{m}$ ).

in Figs. 6a and 6b should be viewed as rough estimates because of the limitations on the depth of analysis and detection limits of EDS.

#### 4. Conclusions

This study has revealed that attainment of equilibrium is concentration-dependent and that increasing sorption temperature leads to a delay in achieving equilibrium. According to the diffusion analysis based on the Boyd equation, the external transport (film diffusion) is more effective in determining the rate of sorption than interlayer diffusion. The sorption data are adequately described by the Freundlich isotherm model, and the sorption process appears to be endothermic. Spot EDS analysis has shown that montmorillonite fractions in natural bentonite are more effective in  $\text{Co}^{2+}$  fixation than cristobalite fractions, and the localization of the signal of adsorbed  $\text{Co}^{2+}$  was also verified by EDS mapping. Based on XRPD analysis, the sorption process was seen to affect the humidity conditions of the interlayer space of the clay.

#### References

- [1] N.M. Nagy, J. Kónya, I. Kónya, *Colloids Surf. A* 137 (1998) 243.
- [2] M.H. Baik, K.J. Lee, *Sep. Sci. Technol.* 30 (1995) 247.
- [3] S.A. Khan, R.U. Rehman, M.A. Khan, *J. Radioanal. Nucl. Chem.* 207 (1996) 19.
- [4] T. Shahwan, H.N. Erten, *Radiochim. Acta* 89 (2001) 799.
- [5] S.A. Khan, *J. Radioanal. Nucl. Chem.* 258 (2003) 3.
- [6] S. Triantafyllou, E. Christodoulou, P. Neou-Syngouna, *Clays Clay Miner.* 47 (1999) 567.
- [7] G. Seren, Y. Bakircioglu, F. Coban, S. Akman, *Fresenius Environ. Bull.* 10 (2001) 296.
- [8] I.N. Levine, *Physical Chemistry*, third ed., McGraw-Hill, 1988, p. 537.
- [9] M. Sarkar, P.K. Acharya, B. Bhattacharya, *J. Colloid Interface Sci.* 266 (2003) 28.
- [10] D. Akar, T. Shahwan, A.E. Eroglu, *Radiochim. Acta* 93 (2005) 477.
- [11] H. Li, B.J. Teppen, C.T. Johnston, S.A. Boyd, *Environ. Sci. Technol.* 38 (2004) 5433.
- [12] T. Shahwan, H.N. Erten, *J. Radioanal. Nucl. Chem.* 253 (2002) 115.
- [13] T. Shahwan, A.C. Atesin, H.N. Erten, A. Zararsiz, *J. Radioanal. Nucl. Chem.* 254 (2002) 563.
- [14] M. Auboiroux, P. Baillif, J.C. Touray, F. Bergaya, *Appl. Clay Sci.* 11 (1996) 117.